NUCLEAR SCIENCE AND ENGINEERING: 56, 360-380 (1975)

Calculational Methods for Nuclear Heating—Part I: Theoretical and Computational Algorithms

M. A. Abdou and C. W. Maynard

University of Wisconsin, Nuclear Engineering Department
Madison, Wisconsin 53706

Received May 6, 1974
Revised October 11, 1974

Methods are investigated for calculating nuclear heating and dose due to the interaction of nuclear radiation with matter. A theoretical model is developed for calculating neutron fluence-to-kerma factors (kerma = kinetic energy released in materials) from basic nuclear data. No major simplifying assumptions are introduced, and the accuracy of the calculated fluence-to-kerma factors depends only on the availability and accuracy of the basic nuclear data. Based on this theoretical model, a computer program called MACK was written to calculate fluence-to-kerma factors from nuclear data in ENDF format.

An algorithm for investigating the validity of the kerma factors by using an integral energy balance was also developed. The validity of the theoretical model and the correctness of the computation of the kerma factors obtained in the present work were verified through the use of this algorithm. Comparison of these kerma-factor results with previous work showed that they provide a considerable improvement in kerma-factor and nuclear-heating calculations. It is also shown that there is currently some inconsistency in preserving the energy between the basic neutron interaction data and the gamma-ray production data. It is suggested that the photon-production matrix be processed simultaneously with the neutron kerma factors to ensure consistency.

I. INTRODUCTION

The calculation of the heat-generation rate and dose due to the interaction of nuclear radiation with matter is of prime importance in practically any nuclear system. In fission reactors, the energy released in the fission reaction is the major contribution to the heat generation. The energy released in the fission reaction is known, and most of it is deposited locally; therefore, the calculation of the heat generation rate in the fission reactor core can be easily determined once the fission rate is known. The contribution to energy deposition from other types of neutron reactions, secondary gamma rays, etc., is usually about 10% of the total and can be calculated by using some simplifying assumptions.

On the other hand, in the absence of fissionable materials, such as in fusion systems or fission reactor shields, the high-energy neutrons can undergo a variety of reactions, and the energy release by each reaction type must be calculated accurately. In this paper, theoretical and computational models are developed for the calculation of energy deposition from basic nuclear data for all neutron reaction types in any energy range.

For the purposes of calculation, the heating rate due to neutron reactions with nuclei of the target material is divided into two types of contribution: (a) heat generated by neutron reactions, and (b) heat generated by the absorption of secondary gamma radiation produced by these neutron reactions. As an example, consider the (n,p) reaction. The energy deposition of the first type is the kinetic energy of (a) the recoil nucleus, (b) the proton emitted, and (c) any charged particle (e.g., β^-) that may be emitted from the activated residual nucleus. The energy deposition by the gamma photons emitted is treated separately.

Heating by neutrons at any spatial point can be expressed as

$$H(\boldsymbol{r}) = \int \phi(\boldsymbol{r}, E) \sum_j \sum_i N_j(\boldsymbol{r})\, \sigma_{ij}(E) E_{ij}(E) dE \quad [\text{eV}/(\text{cm}^3\ \text{sec})] \quad , \tag{1}$$

where

$\phi(\boldsymbol{r}, E)$ = neutron flux at spatial point $\boldsymbol{r}$ and energy E

$N_j(\boldsymbol{r})$ = number density of element j at point $\boldsymbol{r}$ (atom/cm^3)

$\sigma_{ij}(E)$ = microscopic cross section of element j for reaction i at neutron energy E (cm^2/atom)

$E_{ij}(E)$ = energy deposited per reaction i in element j (eV).

The units have been chosen as those normally employed in nuclear calculations.

The terms k_{ij} and k_j, defined as

$$k_{ij}(E) = \sigma_{ij}(E)\, E_{ij}(E) \tag{2}$$

$$k_j(E) = \sum_i k_{ij}(E) \quad , \tag{3}$$

are flux and density independent. The heating rates can therefore be calculated from particle transport results for any system if the factors k_j are predetermined for all materials in the system.

The term k_{ij} represents the microscopic kerma factor for reaction i in element j. The term "kerma" is an acronym for kinetic energy released in materials. The phrase "fluence-to-kerma factors" was introduced by the International Commission on Radiological Units and Measurements[1] and is widely used.[2-7] The term "kerma factor" will be used throughout this paper and is defined by Eqs. (1) and (3); E_{ij} is defined as follows.

The term $E_{ij}(E)$ represents the energy released in element j per reaction i induced by a neutron of energy E. The energy release considered here is the energy assumed to be deposited locally, i.e., within a negligible distance from the site of the reaction. This implies that E_{ij} is the sum of the kinetic energies of the recoil nuclei, charged particles emitted, and charged particles produced by radioactive decay of the residual nucleus and such other processes as internal conversion. The addition of the contribution from radioactive decay to energy deposition depends on the type of calculation performed: time dependent or steady state; this comment is elaborated on later in this paper.

The gamma-ray kerma factors are defined in a similar manner and can be determined from

$$k_\gamma^j = \sigma_{pe}^j E + \sigma_{pp}^j (E - 1.02) + \sigma_{ca}^j E \quad , \tag{4}$$

where

$k_\gamma^j(E)$ = gamma-ray kerma factor for element j [MeV (cm^2/atom)]

E = photon energy (MeV)

σ_{pe}^j = photoelectric microscopic cross section for element j (cm^2/atom)

σ_{ca}^j = Compton microscopic absorption cross section for element j (cm^2/atom)

σ_{pp}^j = pair production microscopic cross section for element j (cm^2/atom).

In pair production, 1.02 MeV (two electron masses) of the photon energy is not available for local heat deposition. The two 0.51-MeV photons produced by the pair are accounted for in the transfer cross sections of gamma-ray-energy multigroup cross-section sets; hence, the energy balance is maintained. Implicit in the use of Eq. (4) is the assumption that photoelectric, pair production, and Compton scattering are the only processes that contribute to energy deposition; all other possible processes are assumed negligible.

The evaluation of gamma-ray kerma factors [Eq. (4)] is straightforward and is usually performed by the codes which generate multigroup photon cross sections such as MUG (Ref. 8) and GAMMA (Ref. 9). Therefore, gamma-ray kerma-factor calculations present no problem at present.

[1] *Radiation Quantities and Units*, Handbook 84, Compiled by the Commission on Radiological Units and Measurements, National Bureau of Standards (1962).

[2] M. L. RANDOLPH, *Rad. Res.*, **7**, 47 (1957).

[3] F. S. WILLIAMSON and P. MITACEK, Jr., "Calculations of Kerma Due to Fast Neutrons in Tissue-Like Materials," *Proc. Symp. Neutron Monitoring Radiological Protection*, p. 17, International Atomic Energy Agency, Vienna (1967).

[4] J. A. AUXIER and W. S. SNYDER, "The Calculation of Kerma as a Function of Neutron Energy," ORNL-4168, Oak Ridge National Laboratory (1967).

[5] R. L. BACK and R. S. CASWELL, *Rad. Res.*, **35**, 1 (1968).

[6] J. J. RITTS, M. SOLOMITO, and P. N. STEVENS, *Nucl. Appl. Technol.*, **7**, 89 (1969).

[7] J. J. RITTS, M. SOLOMITO, and D. STEINER, "Kerma Factors and Secondary Gamma-Ray Sources for Some Elements of Interest in Thermonuclear Blanket Assemblies," ORNL-TM-2564, Oak Ridge National Laboratory (1970).

[8] J. R. KNIGHT and F. R. MYNATT, "MUG: A Program for Generating Multigroup Photon Cross Sections," CTC-17, Computer Technology Center, Union Carbide Corporation (Jan. 1970).

[9] M. J. STANLEY, "Klein-Nishina Photon Cross Sections; Program GAMMA," APEX-487, General Electric Company (May 1959).

The calculation of neutron kerma factors, on the other hand, is complicated by the variety of reactions that a neutron can undergo and the emission of more than one particle in many of these reactions. However, the kinematics and theory are still simple, and the limitation on the accuracy of a neutron kerma calculation is determined by the availability and accuracy of the nuclear data.

Prior to the work reported here, several efforts were made to calculate kerma factors. Some of these are reported in Refs. 2 through 7. However, these efforts were directed mostly toward calculating kerma for elements that are major constituents in the human body. Furthermore, they involved several simplifying assumptions, such as neglecting inelastic scattering entirely, anisotropy of elastic scattering, and several others. The work of Back and Caswell[5] and Ritts et al.[6] included a larger number of reactions and in this sense was an improvement over all preceding work. In the work of Ritts et al., kerma factors were calculated for 11 elemental constituents of the human body. This work was extended[7] to determine the kerma for seven elements of interest in fusion-reactor blankets. However, in their work Ritts et al. did not have a general format or algorithm for calculating kerma, and the same effort had to be duplicated for each material or for a new evaluation of the basic data for the same material. In addition, their work involved some approximations in calculating the secondary neutron energy distribution and the excitation of residual nuclei in nonelastic reactions. The work of Back and Caswell[5] was limited to hydrogen, nitrogen, carbon, and oxygen.

The theoretical models derived in this work for calculating neutron kerma factors are based on accurate solutions of the kinematics equations for all neutron reaction types. A computer program called MACK was written to use these models in calculating kerma factors from nuclear data in the Evaluated Nuclear Data File (ENDF) format.[10,11] The ENDF/B is used to store and retrieve evaluated sets of neutron and photon cross sections. The ENDF formats are versatile and flexible enough that almost any type of neutron interaction mechanism can be accurately described. Furthermore, the nuclear data in the ENDF/B library are continuously revised, re-evaluated, and updated, thus providing the most suitable up-to-date nuclear data library.

[10]"Data Formats and Procedures for the ENDF Neutron Cross Section Library," M. K. DRAKE, Ed., BNL-50274, Brookhaven National Laboratory (Oct. 1970).

[11]O. OZER and D. GARBER, "ENDF/B Summary Documentation," BNL-17541 and ENDF-201, Brookhaven National Laboratory (July 1973).

In Sec. II, theoretical and computational models are developed for calculating kerma factors from basic nuclear data for all neutron reaction types in any energy range. Based on these developments, kerma factors are calculated for many materials of interest; samples of the numerical results are given in Sec. III. A scheme for investigating the validity of the kerma-factor values is developed in Sec. IV and is then applied to the results of the present work. The relationship between these parameters and photon production is also examined. In Sec. V our results are then compared with those obtained in previous work.

Section VI briefly summarizes the important conclusions. In two other papers to follow (Parts II and III), the results presented in this paper are applied to fusion reactors and neutron dosimetry. Part II (Ref. 12) also includes a sensitivity study of neutron heating to basic nuclear data.

II. THEORY FOR KERMA-FACTOR CALCULATIONS

The microscopic kerma factor can be determined from an energy balance for reactions induced by a neutron of energy, E. Thus,

$$k_n(E) = \sigma_t(E)\left(E + \sum_i \frac{\sigma_i}{\sigma_t} Q_i + \sum_{i'} \frac{\sigma_{i'}}{\sigma_t} E_{Di'} - \sum_j \frac{\sigma_j}{\sigma_t} \overline{E}_{n,j} - \sum_g \frac{\sigma_g}{\sigma_t} \overline{E}_{g,\gamma}\right) , \quad (5)$$

where σ_t is the total microscopic collision cross section, and the terms in parentheses are the energies contributed or taken by a particular reaction weighted by the relative probability of the reaction, i.e., by the cross-section ratios. The first term is the energy of the incident neutron times the probability that a collision occurred which is certain; Q_i is the energy resulting from mass conversion in reaction i, $\underline{E}_{Di'}$ is the average decay energy per reaction i', $\overline{E}_{n,j}$ is the average secondary neutron energy per reaction j, and $\overline{E}_{g,\gamma}$ is the average gamma-ray energy per gamma-ray-producing reaction, g. The last term is related to the gamma-ray production cross section $\sigma_p(E, E_\gamma)$ by

$$\sum_g \sigma_g(E)\,\overline{E}_{g,\gamma} = \int \sigma_p(E, E_\gamma)\, E_\gamma\, dE_\gamma \quad . \quad (6)$$

From Eq. (5), calculation of neutron kerma factors requires knowledge of the following:

1. reaction cross sections
2. reaction Q values

[12]M. A. ABDOU and C. W. MAYNARD, *Nucl. Sci. Eng.*, **56**, 381 (1975).

3. secondary neutron-energy distributions
4. energies of photons emitted
5. energy deposition per reaction from radioactive decay.

Note that detailed secondary neutron and photon spectra are not needed for accurate kerma calculation if the (average) total energy of secondary neutrons and photons per total collision can be obtained otherwise.

Nuclear data can generally be classified into three types: (a) neutron interaction, (b) gamma-ray production, and (c) gamma-ray interaction data. Only the first two types are needed in calculating neutron kerma factors. Neutron interaction data include neutron cross sections for the various reactions and secondary neutron energy and angular distributions. Gamma-ray production data provide the information about energy and angular distributions and yields of the secondary photons from neutron-induced reactions. If the data available of both types for a material are complete, the calculation of k_n is straightforward. However, a close look at the currently available and evaluated data (such as in ENDF/B and United Kingdom Atomic Energy Agency Nuclear Data Libraries[13]) reveals that the gamma-ray production data are less well known than the neutron interaction data. However, the information about gamma-ray production required for calculating k_n can be obtained from the neutron interaction data and the solution of the kinematics equations for neutron interactions. These kinematic equations are solved next, and the contribution to the kerma factor from each significant reaction is obtained.

Equations (2) and (3) clearly indicate that the basic quantity to be calculated for generating kerma factors is the energy released by each type of reaction, E_{ij}. Since we need to consider kerma for an element, the subscript j will be dropped. Furthermore, since one reaction at a time is considered in the following discussion, the subscript i will also be dropped unless a distinction is needed. Throughout this section, several quantities are used as defined below (for each reaction):

E_r = kinetic energy of the recoil nucleus

E_R = sum of kinetic energies of the recoil nucleus and the charged particles emitted

E_H = total energy release from the reaction considered ($E_H = E_{ij}$)

$A = AWR$ = ratio of the nuclear mass of the element to that of the neutron.

II.A. Reaction Types

For kerma calculation, the nuclear reactions are conveniently classified into the seven types given in Table I. In Table I, MT is the ENDF/B reaction number and LR is a flag used in ENDF/B to allow inclusion of information about the (n, n') part of a combined inelastic reaction (other than gamma-ray emission) by presenting these reactions where MT = 50 to 91 (inelastic scattering to levels and continuum) and using the appropriate MT number in the LR flag field.

The methods used to calculate the energy released by each type of reaction are summarized below. The kinematics are derived from energy and momentum conservations; however, the details are not given here. Since present ENDF data generally extend only to 15 MeV, the energy range required for most applications, contributions to the kerma factors from $(n, 3n)$ reactions and from secondary nuclear reactions caused by charged-

[13] K. PARKER, "The Aldermasten Nuclear Data Library as of May 1963," AWRE 0-70163, U.K. Atomic Weapons Research Establishment (1963).

TABLE I

Reaction Types

	Reaction Type	ENDF/B Reaction Number, MT
(n, n)	Elastic	2
$(n, n')\gamma$	Inelastic level	51 to 90
$(n, n')\gamma$	Inelastic continuum	91
$(n, mn')\, a_{c_1}, a_{c_2} \ldots$	$(n, mn'$, charged particles), m = 1 or 2	22, 23, 24, 28, and 51 to 91 with flag LR
$(n)\, a_{c_1}, a_{c_2}, a_{c_3} \ldots$	$(n$, charged particles)	103 to 109 700 to 799
(n, γ)	Radiative capture	102
$(n, 2n)$		16

particle products of the primary reaction are neglected.

II.B. Elastic Scattering

The only contribution to kerma from elastic scattering is the deposition of the kinetic energy of the recoil nucleus, E_r:

$$E_H = \overline{E}_r \quad , \tag{7}$$

where E_r is a function of the scattering angle of the neutron. The average recoil energy is obtained by weighting $E_r(\theta)$ by the differential scattering cross section:

$$\overline{E}_r = \frac{2AE}{(A+1)^2}\,(1 - \overline{\cos\,\theta_{cm}}) \quad , \tag{8}$$

where $\overline{\cos(\theta_{cm})}$ = average of the cosine of the center-of-mass scattering angle

$$\overline{\cos(\theta)} = \frac{\int_{-1}^{+1} \mu\,\sigma(\mu, E)\,d\mu}{\int_{-1}^{+1} \sigma(\mu, E)\,d\mu} = F_1 \quad , \tag{9}$$

where

$\mu = \cos\,\theta$

F_1 = first coefficient of the Legendre polynomial expansion of the differential scattering cross section.

II.C. Inelastic-Level Scattering

The average energy of the recoil nucleus is given by

$$\overline{E}_r = E - \overline{E}_{n',1} - E_\lambda \quad , \tag{10}$$

where

E = incident neutron energy

E_λ = energy of the excited level

$\overline{E}_{n',1}$ = average kinetic energy in the laboratory system of the emitted neutron

$$\overline{E}_{n',1} = \frac{2AE}{(A+1)^2}\left[\frac{A^2+1}{2A} - \frac{(A+1)E_\lambda}{2E} + \left(1 - \frac{A+1}{A}\,\frac{E_\lambda}{E}\right)^{1/2} \overline{\cos\,\theta_{cm}}\right] \quad . \tag{11}$$

The energy deposition per inelastic level reaction can be written as

$$E_H = \overline{E}_r + f_c E_\lambda \quad , \tag{12}$$

where f_c is the fraction of E_λ locally converted to heat. For example, if internal conversion competes with gamma-ray emission, then f_c is given by

$$f_c = C_F/(1 + C_F) \quad , \tag{13}$$

where C_F is the internal conversion factor.

II.D. $(n, n')\gamma$ to the Continuum

The average recoil energy is given by

$$\overline{E}_r = E - \overline{E}_{n',1} - \overline{\epsilon} \quad , \tag{14}$$

where $\overline{\epsilon}$ is the average excitation of the residual nucleus. If, for inelastic scattering in the continuum range, neutrons are emitted isotropically, then

$$\overline{\epsilon} = \frac{A^2+1}{A(A+1)}\,E - \frac{A+1}{A}\,\overline{E}_{n',1} \quad . \tag{15}$$

The energy distribution of the secondary neutron, $P(E \rightarrow E')$, can be broken down into partial energy distributions, $f_k(E \rightarrow E')$, where each of the partial distributions can be described by a different analytic representation:

$$P(E \rightarrow E') = \sum_{k=1}^{NK} P_k(E)\, f_k(E \rightarrow E') \quad ,$$

and at a particular incident neutron energy E,

$$\sum_{k=1}^{NK} P_k(E) = 1 \quad .$$

The ENDF format allows several analytic formulations for the partial energy distributions, $f_k(E \rightarrow E')$.

An expression for $E_{n',1}$ is evaluated as follows:

$$\overline{E}_{n',1}(E) = \frac{\int_{E'_{min}}^{E'_{max}} E'\,P(E \rightarrow E')\,dE'}{\int_{E'_{min}}^{E'_{max}} P(E \rightarrow E')\,dE'}$$

$$= \sum_{k=1}^{NK} P_k(E) \int_{E'_{min}}^{E'_{max}} E'\,f_k(E \rightarrow E')\,dE'$$

$$= \sum_{k=1}^{NK} P_k(E)\,\overline{E}_{n',1,k} \quad . \tag{16}$$

The analytic form of $\overline{E}_{n',1,k}$ depends on the analytic formulation of $f_k(E \rightarrow E')$.

For the evaporation spectrum

$$f(E \rightarrow E') = \frac{E'}{I}\,\exp[-E'/\theta(E)] \quad ,$$

where I is a normalization constant that depends on E'_{min}, E'_{max}, and θ. The ENDF assumes that $E'_{min} = 0$. Using this assumption, we obtain

$$\overline{E}_{n',1,k} = \theta\,\frac{2\exp(x_1) - [1 + (1+x_1)^2]}{\exp(x_1) - (1 + x_1)} \quad , \tag{17}$$

where

$$x_1 = \frac{E'_{max}}{\theta} \quad .$$

For a simple fission spectrum (Maxwellian),

$$f(E \rightarrow E') = \frac{\sqrt{E'}}{I}\,\exp[-E'/\theta(E)] \quad , \tag{18}$$

and by invoking the assumption that $E'_{min} = 0$, we obtain

$$\overline{E}_{n',1,k} = \theta\left\{\frac{3}{2} - \frac{x_1^{3/2}}{\left[\frac{\sqrt{\pi}}{2}\exp(x_1)\,\mathrm{erf}(\sqrt{x_1}) - \sqrt{x_1}\right]}\right\} \quad . \tag{19}$$

For the other allowable representations of $f_k(E \rightarrow E')$, $E_{n',1}$ can be obtained by numerical integration in Eq. (16).

II.E. (n, n') Charged Particles

In this type of reaction, in addition to the secondary neutrons, the emission of one or two charged particles occurs. The reaction is generally of the form

$$_{Z_1}X^{A_1}(n,n')a_{c_1}, a_{c_2}, \ldots . a_{c_n} \quad , \quad _{Z_2}Y^{A_2} \quad .$$

We define

$$E_R = E_r + E_{a_1} + E_{a_2} + \ldots + E_{a_n} \quad , \tag{20}$$

where

E_r = kinetic energy of recoil nucleus Y

E_{a_i} = kinetic energy of the i'th charged particle.

In kerma calculation we are not concerned with the partition of energy between charged particles and the recoil nucleus since all charged particles (and the "recoil nucleus") will deposit their kinetic energy at or near the site of the collision. This allows us to evaluate E_R by applying only the energy conservation principle

$$\overline{E}_R = E - \overline{E}_{n',1} - |Q_0| - \epsilon_Y \quad , \tag{21}$$

where

Q_0 = Q value for the combined reaction when the residual nucleus is left in the ground state

ϵ_Y = average excitation of the residual nucleus.

Assuming that in an $[(n,n')a_{c_1}, a_{c_2}\ldots a_{c_n}]$ type of reaction the neutron is emitted first, we can evaluate $\overline{E}_{n',1}$ as discussed before for inelastic to discrete or continuum level scattering, depending on the state of the intermediate nucleus left after the emission of the neutron.

If the residual nucleus, after emitting the neutron and charged particles, is left in the isolated level region, E_R and the corresponding kerma factor must be evaluated for each possible level. If the residual nucleus is left in the continuum range (infrequent for reactions induced by neutrons of energy <14 MeV), the evaluation of the average energy of the residual nucleus requires information about the energy spectra of the charged particles emitted. Currently, ENDF/B does not provide such information. In reactions of the type $(n,2n)\,a_{c_1}, a_{c_2}\ldots a_{c_n}$, E_R can be evaluated from the last equation, with $\overline{E}_{n',1}$ as the sum of the average energies of the two neutrons.

The total energy release per reaction, E_H, is the sum of E_R and E_D, where E_D is the contribution to heat deposition by particle emission (usually β^- or β^+) from the decay of the activated residual nucleus. Methods for calculating E_D will be given after a discussion of the kinematics of the other types of reactions.

II.F. Charged-Particle Reactions

The reaction discussed here is of the type

$$_{Z_1}X^{A_1}(n; a_{c_1}, a_{c_2}\ldots a_{c_n})\,_{Z_2}Y^{A_2} \quad ,$$

where a_{c_1}, $a_{c_2}\ldots$ are charged particles, e.g., (n,α), (n,p), $(n,\alpha T)$. The partition of the kinetic energy of the emitted charged particles and the residual nucleus is not needed:

$$E_H = E_R + E_D \quad ,$$

where

$$E_R = E_{a_{c_1}} + E_{a_{c_2}} + E_{a_{c_n}} + E_r \quad .$$

The residual nucleus is frequently left in one of the excited states, and the kerma factor for this type of reaction is the sum of the kerma factors to each level:

$$k = k_0 + k_1 + k_2 + \ldots + k_N + k_{con} \quad , \tag{22}$$

where N is the number of levels and the subscript con denotes continuum.

Denoting E_R and E_H for the i'th level by E_{Ri} and E_{Hi}, respectively, we can write

$$E_{Ri} = E + Q_0 - \epsilon_{Yi} \quad , \tag{23}$$

where

Q_0 = reaction mass Q value (Q value to the ground state)

ϵ_{Yi} = energy of level i excited in the residual nucleus.

The quantities E_{Hi} and k_i are

$$E_{Hi} = E_{Ri} + E_{di} \tag{24}$$

and

$$k_i = \sigma_i E_{Hi} \quad , \tag{25}$$

where

σ_i = reaction cross section for the i'th excited state

E_{di} = contribution to energy deposition by radioactive decay of the i'th level (except gamma-ray emission).

The expression for k can be easily given as

$$k = \sigma[(E + Q_0) - E_\gamma + E_D] \quad , \tag{26}$$

where

$$E_\gamma = P_1\epsilon_1 + P_2\epsilon_2 + \ldots + P_N\epsilon_N \tag{27}$$

$$E_D = P_0E_{d0} + P_1E_{d1} + \ldots + P_NE_{dN} \quad , \tag{28}$$

$$\sigma = \sum_i \sigma_i$$

ϵ_i = energy of the i'th level

$P_i = \sigma_i/\sigma$ = probability that the i'th level will be excited, given that a reaction has occurred.

If other processes compete with gamma-ray emission, the ϵ_i's in the above expression should be adjusted. For example, if internal conversion competes with gamma-ray emission from the i'th level, then ϵ_i should be adjusted to

$$\epsilon_{im} = \epsilon_i(1 - f_{ci}) \quad , \tag{29}$$

with

$$f_{ci} = C_{Fi}/(1 + C_{Fi}) \quad , \tag{30}$$

where C_{Fi} is the internal conversion factor for the i'th level.

II.G. Radiative Capture

The kinetic energy of the recoil nucleus in an (n, γ) reaction is obtained by momentum and energy balances, which yield

$$E_r = E + Q + M_rc^2 - M_rc^2\left[1 + \frac{2\left(Q + \frac{AE}{A+1}\right)}{M_rc^2}\right]^{1/2} \quad , \tag{31}$$

where

M_rc^2 = mass of the residual nucleus in energy units $= (A + 1)m_nc^2 - Q$

m_nc^2 = energy equivalent of the neutron mass (939.512 MeV).

If radioactive decay occurs after an (n, γ) reaction, E_H is the sum of E_r and E_D.

II.H. $(n, 2n)$ Reaction

The $(n,2n)$ reactions followed by charged-particle emission were treated previously. We are concerned here with $(n,2n)$ reactions followed by gamma-ray emission (or internal conversion). The recoil energy of the nucleus is given by

$$\bar{E}_r = E - (\bar{E}_{n_1,1} + \bar{E}_{n_2,1}) - B - \bar{\epsilon}_{A-1} \quad , \tag{32}$$

where

$\bar{E}_{n_1,1}$ = average kinetic energy of the first neutron emitted in the laboratory system

$\bar{E}_{n_2,1}$ = average kinetic energy of the second neutron emitted in the laboratory system

B = binding energy of the last neutron in the target nucleus

$\bar{\epsilon}_{A-1}$ = average excitation of the residual nucleus.

Assuming that the $(n,2n)$ reaction is a two-step process, i.e., one neutron followed by another with isotropic emission, we show $\bar{\epsilon}_{A-1}$ to be

$$\bar{\epsilon}_{A-1} = \frac{A^2 + 2}{A(A+1)}E - B - \frac{1}{A-1} \times \left(\frac{A^2 - 2}{A}\bar{E}_{n_1,1} + A\,\bar{E}_{n_2,1}\right) \quad . \tag{33}$$

The average energy of each neutron can be calculated from the energy distribution of that neutron, as done previously. Evaluation of $\bar{\epsilon}_{A-1}$ requires knowledge of the energy distribution for each of the two neutrons. If only the combined energy spectrum of the two neutrons is known, the calculation of $\bar{E}_r$ without approximation is possible only when the residual nucleus is left in the ground state. The contribution to the energy deposition from internal conversion and radioactive decay, if any, should be added to $\bar{E}_r$ to get $\bar{E}_H$.

II.I. Kerma Factors for a Mixture of Isotopes

The kerma factors for a mixture of isotopes can be obtained by summing the macroscopic kerma factors for all isotopes present in the mixture. For example, consider an element or a mixture that consists of several isotopes. The kerma factors for the mixture are

$$K_m = \sum_j K_j \tag{34}$$

and

$$K_j = N_jk_j \quad , \tag{35}$$

where

k_j = microscopic kerma factor for the j'th isotope in the mixture

N_j = number density of the j'th isotope in the mixture

K_m = macroscopic kerma factor for the mixture.

For some natural elements (e.g., molybdenum, iron, etc.) which consist of several isotopes, it may be desirable to evaluate directly the kerma

factors for the element without calculating the K_j's This requires appropriate definitions of the various physical quantities involved in kerma calculations. The guiding rule is that the definitions of the physical quantities and the equations for K_m must reproduce Eq. (34). A definition of the Q value for a mixture of isotopes is discussed below and is followed by a discussion of other quantities.

Consider a reaction that occurs in one or more of these isotopes; then, by definition,

$$Q \text{ value for the } j\text{'th isotope} = Q_j = E_{R_j} - E \quad , \tag{36}$$

where E_{R_j} is the kinetic energy of the product particles and E is the kinetic energy of the colliding particles. Since the kinetic energy released in the mixture must equal the sum of the kinetic energies released in the various isotopes in the mixture, we can write

$$N_m \sigma_m E_{R_m} = \sum_j N_j \sigma_j E_{R_j} \quad , \tag{37}$$

where E_{R_m} is the kinetic energy of the product particles per reaction in the mixture. Making use of the definitions of Q_j and σ_m, which is

$$\sigma_m = \frac{1}{N_m} \sum_j N_j \sigma_j \quad ,$$

we can rewrite Eq. (37) as

$$E_{R_m} - E = \sum_j Q_j \frac{\sigma_j N_j}{\sigma_m N_m} \quad . \tag{38}$$

Since the left side of Eq. (38) is the kinetic energy released by or required for a reaction in the mixture, the right side is recognized as the Q value for the mixture:

$$Q_m = \sum_j Q_j \frac{\sigma_j N_j}{\sigma_m N_m} \quad . \tag{39}$$

Since definition (39) is derived by using only a conservation principle, Eq. (37), and the basic definition of the Q value for an isotope, it is a unique definition compatible with the definition of the Q value for an isotope and should be acceptable for any physics calculation that uses the Q value in its normal definition.

Similar definitions for the various physical quantities for a mixture of isotopes can be developed easily by applying similar arguments. For example, the average energy of a secondary neutron from and the decay energy following a reaction in the mixture can be written as

$$\overline{E}_{n',l,m} = \sum_j \frac{N_j \sigma_j}{N_m \sigma_m} \overline{E}_{n',l,j} \tag{40}$$

$$E_{D,m} = \sum_j \frac{N_j \sigma_j}{N_m \sigma_m} E_{D,j} \quad . \tag{41}$$

An equation for the kerma factor for any reaction in a mixture in the same form as for a single isotope (with the physical quantities involved as defined above) can be written to satisfy Eq. (34). This is no surprise since kerma itself is a physical quantity and Eq. (34) is merely an expression for a physical conservation law. In other words, any definition of the physical quantities for a mixture of isotopes that satisfies the physical laws (e.g., energy and momentum conservation) would necessarily be compatible with Eq. (34).

A special case implicitly included in Eqs. (39), (40), and (41) is a reaction that occurs only in one isotope. In this case, Eq. (40) reduces to

$$\overline{E}_{n',l,m} = \overline{E}_{n',l,J} \quad ,$$

where J is the isotope in which this reaction occurs. An example is inelastic-level scattering where each level belongs to a particular isotope. Therefore, in applying Eq. (11) for a mixture of isotopes, A should be taken as the atomic weight ratio for the particular isotope in which the level considered is excited.

From the above discussion, it can be seen that for single isotopes, energy-independent parameters (e.g., Q value, decay energies, etc.) are energy dependent for a mixture of isotopes because σ_j/σ_m is generally energy dependent for any reaction except the special case of a reaction that occurs only in one isotope.

Another observation worth noting is that kerma calculations cannot be accurately made if nuclear data are available only for the mixture and not for the constituent isotopes. For example, the use of only an abundance-weighted Q value for a reaction such as (n,p) would result in a negative kerma factor for that reaction in an energy range whose width depends on the thresholds of the reaction in and the abundance of the constituent isotopes.

II.J. Energy Deposition Due to Radioactive Decay

Depending on the composition and neutron spectra of the system, heating due to the decay of the activated residual nucleus can be very significant. It is convenient to classify the heating from radioactive decay of the residual nucleus into energy deposition by particle emission and energy release by gamma-ray emission. Very accurate calculations of the decay contribution to the total heating requires accounting for the time dependence and transmutation of the radioactive residual nucleus by neutron interactions. This requires the use of a special-purpose program such as CINDER (Ref. 14). However, if the contribution of radioactive decay is not very large compared with the total heating and if we assume

[14]T. R. ENGLAND, "An Investigation of Fission Product Behavior and Decay Heating in Nuclear Reactors," PhD Thesis, University of Wisconsin (Aug. 1969).

that (a) energy deposition is negligible from radioactive residual nuclei with half-lives greater than an arbitrary cutoff, T_c (e.g., 30 days; note that the mean lifetime increases rapidly as the disentegration energy decreases), and (b) transmutation of residual nuclei can be ignored, (i.e., each residual nucleus decays before it undergoes another nuclear reaction), then heating by radioactive decay is, to a large extent, time independent for steady-state systems operating for periods much longer than T_c. In such cases, it is convenient to add the energy deposition by particle emission to the neutron kerma factors. Energy deposition by gamma-ray emission can be properly accounted for by adding these gamma rays to the secondary gamma-ray production source. Afterheat calculations clearly require more detailed treatment of the time dependence and chain reactions of the decay products.

The most frequent type of decay is by emission of β^- particles. β^+ decay may occur after $(n,2n)$ reactions, and β^- decay after (n,γ), (n,α), (n,p), etc., reactions. Since beta particles are emitted with an energy spectrum, the average kinetic energy of the beta particles, $\overline{E}_\beta$, must be calculated. Previous works in nuclear engineering assumed the average kinetic energy of a beta particle to be 30% of the end-point energy for all isotopes and end-point energies. As shown next, this assumption severely underestimates $\overline{E}_\beta$ in many important cases.

The basic problem in calculating $\overline{E}_\beta$ is the calculation of the energy distribution of the beta particles. Fermi's theory[15] of beta decay predicts the probability of emitting a beta particle with kinetic energy E for end-point energy E_0 to be

$$P(W) = GF(Z,W)(W^2-1)^{1/2}(W_0-W)^2 W \quad , \tag{42}$$

where

$$W = \frac{E(\text{MeV})}{0.51} + 1$$

$$W_0 = \frac{E_0(\text{MeV})}{0.51} + 1 \quad , \tag{43}$$

Z = atomic number

G = quantity independent of W whose actual magnitude is not important in the following discussion.

The $F(Z,W)$ is a complicated function that accounts for the effect of the nuclear coulomb potential on the emitted beta particle. The form of the F factor is discussed in Ref. 15 where more detailed references are given. A relativistic expression for F is

$$F(Z,W) = \left\{\frac{4(1+s/2)}{[\Gamma(3+2s)]^2}\left(\frac{2r}{\hbar/m_0c}\right)^{2s}\right\} \times [(W^2-1)^s \exp(\pi y)\,|\Gamma(1+s+iy)|^2] \quad , \tag{44}$$

where

$$s = [1-(Z/137)^2]^{1/2} - 1 \tag{45}$$

r = nuclear radius

$\hbar/m_0c = 3.86 \times 10^{-11}$ cm

Γ = complex gamma function

$$y = \frac{aZW}{137(W^2-1)^{1/2}} \qquad \begin{matrix} a = +1 \text{ for } \beta^- \text{ decay} \\ a = -1 \text{ for } \beta^+ \text{ decay} \end{matrix} \tag{46}$$

For $|s| \ll 1$, $F(Z,W)$, to a good approximation, is given by

$$F(Z,W) \simeq \frac{2\pi y}{1-\exp(-2\pi y)} \quad , \tag{47}$$

with y as given in Eq. (46).

The average energy of a beta particle, $\overline{E}_\beta$, can be written as

$$\overline{E}_\beta\,(\text{MeV}) = 0.51\,\frac{\int_1^{W_0}(W-1)P(W)dW}{\int_1^{W_0}P(W)dW} \quad , \tag{48}$$

with $P(W)$ given by Eq. (42) and $F(Z,W)$ by Eq. (44). The nonrelativistic approximation, Eq. (47), results in an error of <2% in evaluating $\overline{E}_\beta$ for $Z < 40$. For $Z = 0$, $F(Z,W)$ is unity.

Equation (48) was evaluated numerically by using Eq. (47) for $F(Z,W)$. The average beta-particle kinetic energy was tabulated as a function of the atomic number and the end-point energy for both β^- and β^+ in Appendix C of Ref. 16. The ratio, R, of $\overline{E}_\beta$ to E_0 is also tabulated there and is given here in Tables II and III for $Z = 10$ for β^- and β^+ decay, respectively.

Several conclusions can be drawn from investigating the ratio R. The results show that R is generally an increasing function of E_0 and is always >30% for E_0 greater than ~0.5 MeV. It increases rapidly with E_0 and Z up to an E_0 of ~3 MeV, after which it varies more slowly. In Fig. 1, R is plotted as a function of E_0 for $Z = 30$

[15] R. D. EVANS, *The Atomic Nucleus*, McGraw-Hill Book Company, New York (1955).

[16] M. A. ABDOU, C. W. MAYNARD, and R. Q. WRIGHT, "MACK: A Computer Program to Calculate Neutron Energy Release Parameters (Fluence-to-Kerma Factors) and Multigroup Neutron Reaction Cross Sections from Nuclear Data in ENDF Format," ORNL-TM-3994, Oak Ridge National Laboratory (July 1973).

for β^- and β^+ compared with R for $Z=0$ for which the coulomb correction is not included. For each end-point energy, R decreases for β^- and increases for β^+ when the nuclear coulomb effect is taken into consideration. The change in R for both β^- and β^+ is more pronounced at smaller E_0. These observations can be explained as follows: The nuclear coulomb potential represents a potential well for the electrons and a barrier for the positrons. Therefore, in β^- decay a surplus of low-energy electrons is produced, resulting in a lower R. For β^+ decay, $F(Z,W)$ of Eq. (47) is

TABLE II

β^- Decay: Average Electron Kinetic Energy for $Z = 10$

E_0 (MeV)	$\overline{E}$ (MeV)	$\overline{E}/E_0$ (×100)
0.01	0.0025	25.4983
0.02	0.0052	26.1592
0.03	0.0080	26.7371
0.04	0.0109	27.2362
0.05	0.0138	27.6735
0.06	0.0168	28.0636
0.07	0.0199	28.4154
0.08	0.0230	28.7374
0.09	0.0261	29.0338
0.10	0.0293	29.3098
0.20	0.0628	31.3860
0.30	0.0985	32.8434
0.40	0.1360	34.0025
0.50	0.1749	34.9760
0.60	0.2149	35.8187
0.70	0.2559	36.5615
0.80	0.2978	37.2244
0.90	0.3404	37.8219
1.00	0.3836	38.3638
1.50	0.6071	40.4751
2.00	0.8388	41.9386
2.50	1.0754	43.0154
3.00	1.3152	43.8409
3.50	1.5573	44.4936
4.00	1.8009	45.0220
4.50	2.0456	45.4587
5.00	2.2913	45.8257
5.50	2.5376	46.1382
6.00	2.7845	46.4075
6.50	3.0317	46.6419
7.00	3.2793	46.8477
7.50	3.5272	47.0299
8.00	3.7754	47.1923
8.50	4.0237	47.3380
9.00	4.2722	47.4693
9.50	4.5209	47.5883
10.00	4.7697	47.6967
11.00	5.2675	47.8867
12.00	5.7657	48.0479
13.00	6.2642	48.1863
14.00	6.7629	48.3064
15.00	7.2617	48.4116
16.00	7.7607	48.5045
17.00	8.2598	48.5872
18.00	8.7590	48.6612

TABLE III

β^+ Decay: Average Positron Kinetic Energy for $Z = 10$

E_0 (MeV)	$\overline{E}$ (MeV)	$\overline{E}/E_0$ (×100)
0.01	0.0049	49.4465
0.02	0.0091	45.6920
0.03	0.0132	43.8656
0.04	0.0171	42.7409
0.05	0.0210	41.9675
0.06	0.0248	41.4004
0.07	0.0287	40.9668
0.08	0.0325	40.6257
0.09	0.0363	40.3516
0.10	0.0401	40.1281
0.20	0.0784	39.1900
0.30	0.1173	39.1006
0.40	0.1570	39.2604
0.50	0.1976	39.5145
0.60	0.2388	39.8060
0.70	0.2808	40.1094
0.80	0.3233	40.4123
0.90	0.3664	40.7082
1.00	0.4099	40.9940
1.50	0.6336	42.2427
2.00	0.8644	43.2182
2.50	1.0996	43.9847
3.00	1.3381	44.6047
3.50	1.5789	45.1101
4.00	1.8212	45.5304
4.50	2.0648	45.8853
5.00	2.3094	46.1886
5.50	2.5548	46.4507
6.00	2.8008	46.6794
6.50	3.0472	46.8806
7.00	3.2941	47.0590
7.50	3.5414	47.2182
8.00	3.7889	47.3612
8.50	4.0367	47.4902
9.00	4.2847	47.6073
9.50	4.5328	47.7140
10.00	4.7812	47.8116
11.00	5.2782	47.9839
12.00	5.7757	48.1311
13.00	6.2736	48.2584
14.00	6.7717	48.3694
15.00	7.2701	48.4672
16.00	7.7686	48.5539
17.00	8.2673	48.6314
18.00	8.7662	48.7010

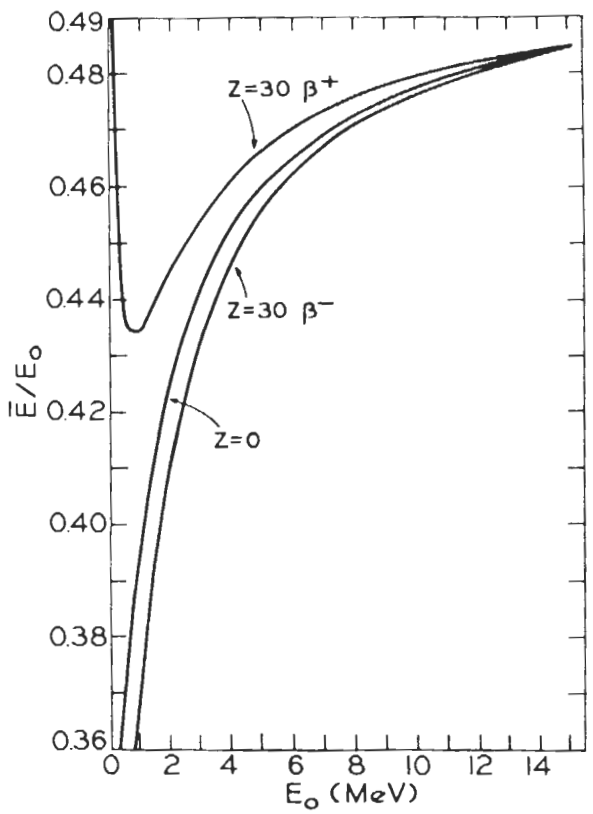

Fig. 1. Ratio of average kinetic energy, $\bar{R}$, of beta particle to the end-point energy of the beta spectrum for $Z = 0$ (no coulomb correction) and $Z = 30$.

$\simeq 2\pi|y|\exp(-2\pi|y|)$ for low-energy positrons. This is a typical barrier transmission factor. Since $|y|$ increases as Z increases and E decreases, the nuclear coulomb effect is most noticeable at high Z and low E. The barrier transmission factor nearly eliminates the emission of low-energy positrons, resulting in a higher R. At very low E_0, the β^+ spectrum is almost nonzero only in the neighborhood of E_0; therefore, R approaches unity as E_0 tends to zero. For isotopes with two or more beta-spectra with different end-point energies, $\bar{E}_\beta$ must be calculated separately for each spectrum and summed weighted by the intensities.

As an example of calculating the contribution to the kerma factor from radioactive decay, consider radiative capture in ^{7}Li:

$$^7\text{Li}(n,\gamma)^8\text{Li} \xrightarrow[T_{1/2} = 0.84\,s]{\beta^-} {}^8\text{Be} \rightarrow 2\alpha \quad .$$

Lithium-8 decays by a 100% intensity beta spectrum to the 2.90-MeV level of ^{8}Be which disintegrates immediately to two alpha particles. Q_β and $Q_{2\alpha}$ are calculated as 16.002 and 0.095 MeV, respectively. Hence, the end-point beta kinetic energy is 13.102, and each alpha particle has a kinetic energy equal to 1.497 MeV. By numerical integration of Eq. (48) for $Z = 3$, we get $\bar{E}_\beta = 6.315$ MeV. Hence, the contribution from radioactive decay per (n,γ) reaction in ^{7}Li is 9.31 MeV. Incidentally, the Q value for the (n,γ) reaction in ^{7}Li is 2.032 MeV; thus, the kerma factor for that reaction is dominated by the contribution from the decay of the activated residual nucleus.

The average energy of the beta decay is not usually given in the table of isotopes[17] or in other compilations for radioisotopes. The beta end-point energy, relative intensities, fraction of electron capture, alpha-particle energies, half-lives, and other required information are usually given in such compilations. This suggests the need to generate a library for the average energy release from radioactive decay for all reactions and isotopes of importance. Such a library not only would be useful for adding the contribution of radioactive decay to kerma factors but also would provide necessary information for calculating decay heat in nuclear devices. It is also suggested that the average energy release from radioactive decay following a nuclear reaction should be specified in ENDF/B File 1, section 453.

II.K. MACK Program

The MACK program[16] was written by the authors to calculate pointwise neutron kerma factors at an arbitrary energy mesh from nuclear data in ENDF format.[10,11] The program processes all reactions significant to energy deposition and recognizes all the multiplicity of data formats currently allowed by ENDF/B. The code makes full use of the kinematics equations solved in this paper. As we introduced no significant approximations into these solutions, the limit on the accuracy of kerma-factor calculations is set only by the availability and adequacy of the required nuclear data.

In addition, the MACK program calculates energy-group kerma factors and group cross sections by reaction averaged over an arbitrary input weighting function or any of several "built-in" functions for any desired group structure. An efficient treatment of the resonance region was built into the program to calculate the contribution to cross sections from the resolved and unresolved resonance parameters, including the Doppler effect. A calculational flow chart of the MACK program is given in Fig. 2.

The pointwise cross sections, pointwise kerma factors, energy-group cross sections, and kerma

[17] C. M. LEDERER, J. M. HOLLANDER, and I. PERLMAN, *Table of Isotopes*, 6th ed., John Wiley and Sons, New York (1967).

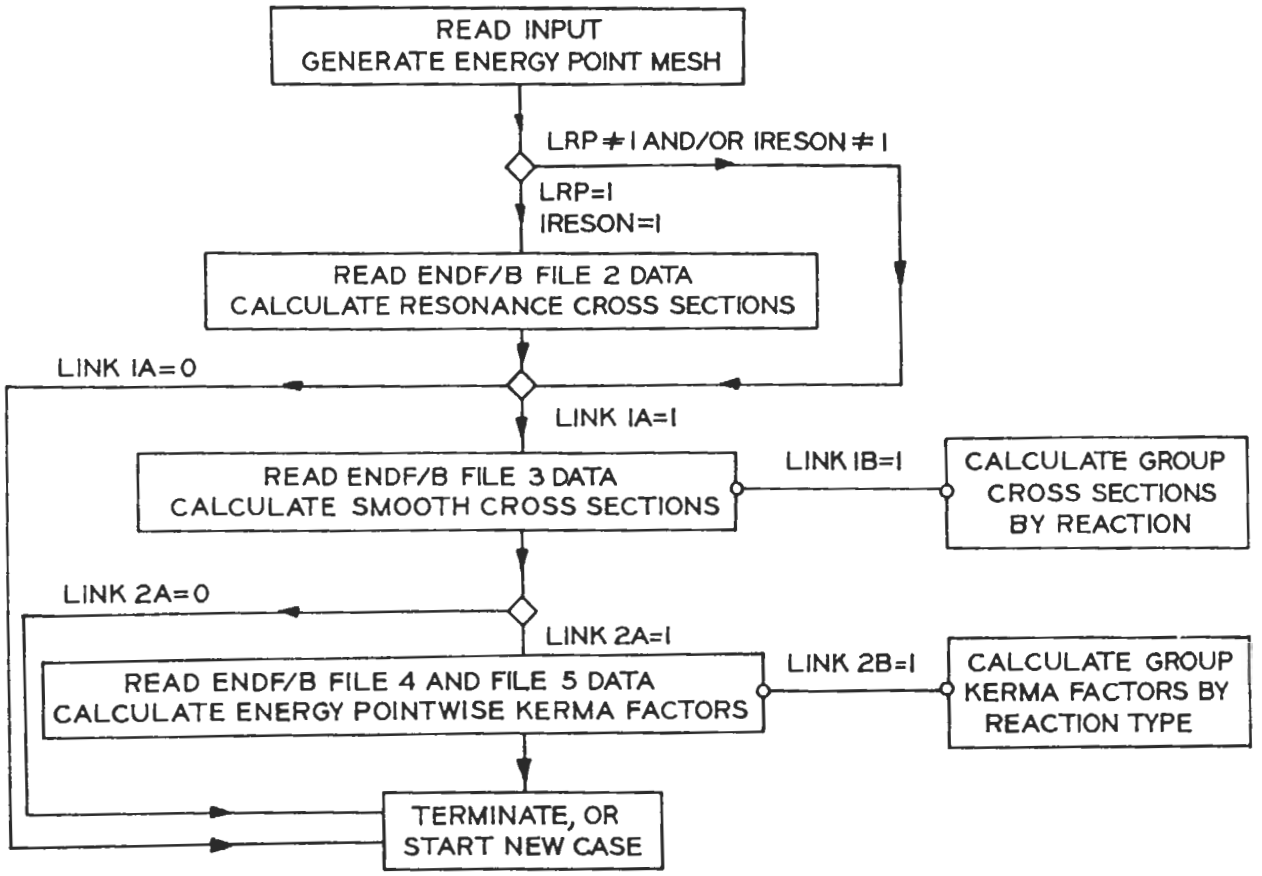

Fig. 2. Calculational flow chart for program MACK.

factors can be printed, punched, and saved on tape for individual reactions and the sum as selected by input. The pointwise kerma factors by reaction and sum can be used for inclusion in the ENDF/B evaluation for the nuclide with *MT* numbers in the 300 series.[10,11] The output group kerma factors and partial cross sections are in a form suitable for use as "activity cross-section tables" in the present one-, two-, or three-dimensional transport codes[18-20] for calculating heating rates and reaction rates of interest (e.g., helium and hydrogen production).

III. RESULTS

Samples of the neutron fluence-to-kerma factors calculated in the present work are shown in Figs. 3 through 10. All the calculations were performed with the MACK program (described earlier) using ENDF/B data. For clarity, some of the resonance details of the kerma factors were

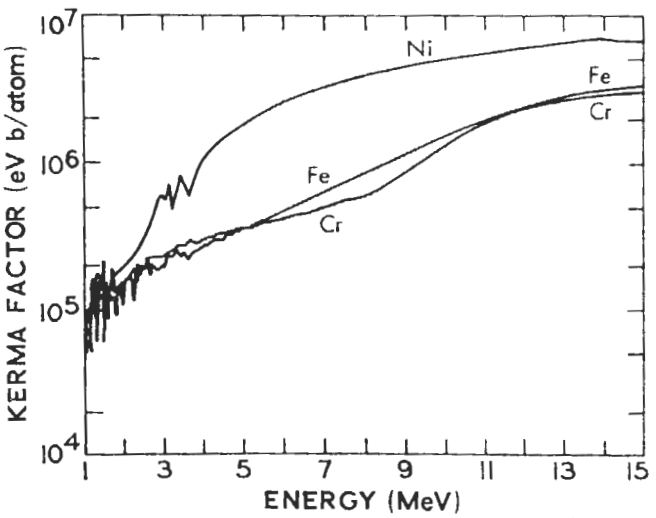

Fig. 3. Neutron kerma factor for iron, chromium, and nickel.

[18] W. W. ENGLE, Jr., "A User's Manual for ANISN," K-1693, Oak Ridge Gaseous Diffusion Plant (Mar. 1967).
[19] F. R. MYNATT, "A User's Manual for DOT," K-1694, Oak Ridge Gaseous Diffusion Plant (1967).
[20] E. A. STRAKER et al., "The Morse Code—A Multigroup Neutron and Gamma Ray Monte Carlo Transport Code," ORNL-4585, Oak Ridge National Laboratory (1970).

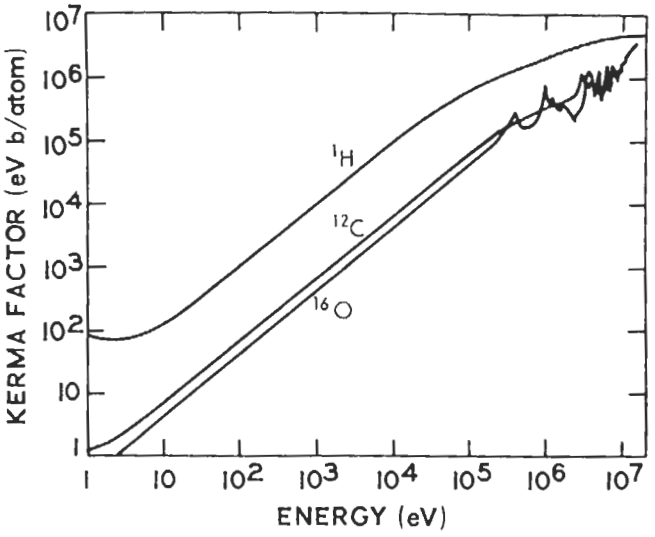

Fig. 4. Neutron kerma factor for ^{1}H, ^{12}C, and ^{16}O.

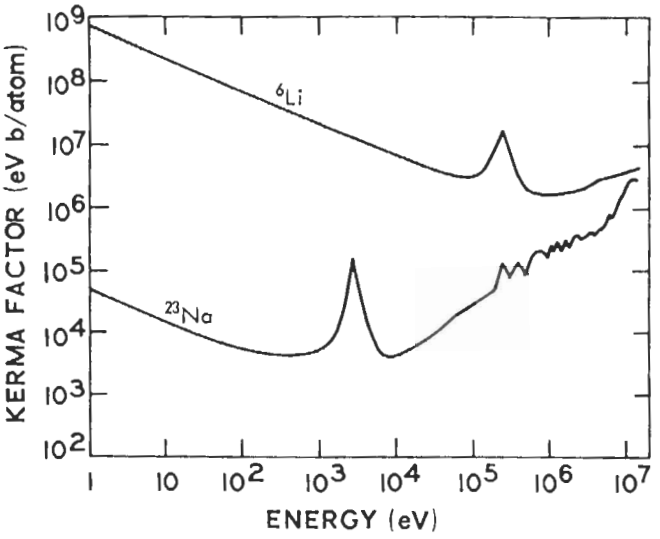

Fig. 6. Neutron kerma factor for ^{6}Li and ^{23}Na.

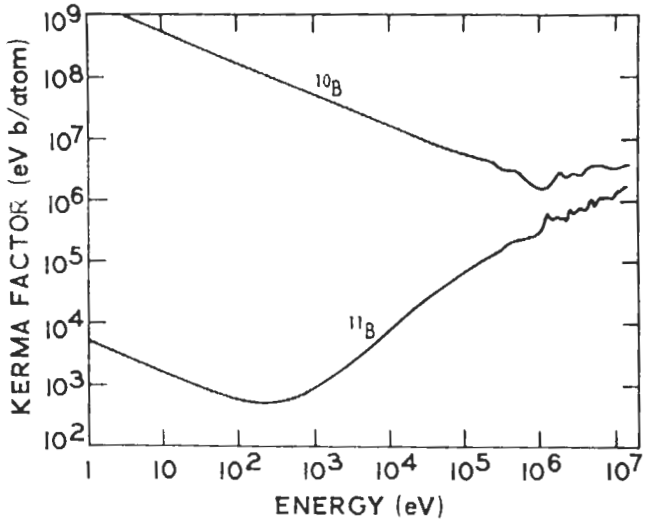

Fig. 5. Neutron kerma factor for ^{10}B and ^{11}B.

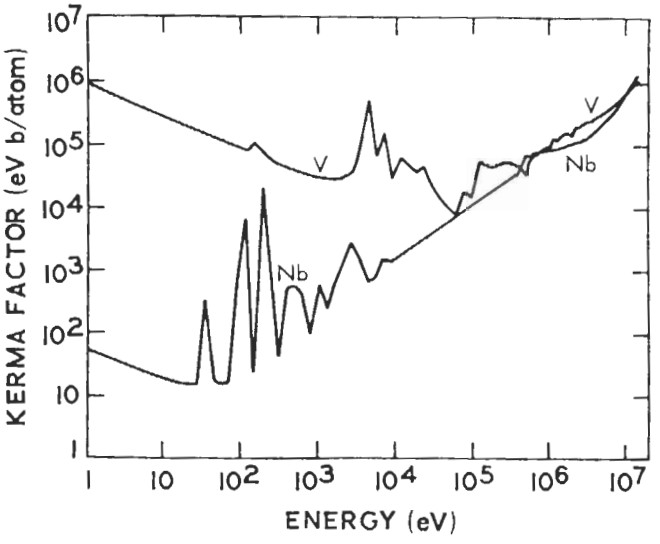

Fig. 7. Neutron kerma factor for vandium and niobium.

smoothed in these graphs. The materials chosen for presentation here are those of common interest in shielding, in fusion reactors, and in calculating the dose to the human body.

The reader is cautioned that in many instances it is difficult to draw conclusions about "energy multiplication" and relative magnitude of total heating rates in various materials by comparing the neutron kerma factors alone. Nuclear heating is a function of the nuclide atomic densities, neutron and gamma-ray flux spectra, and neutron and gamma-ray kerma factors. The ratio of neutron to gamma-ray heating varies considerably from material to material. Materials that attenuate neutrons mostly through inelastic-scattering reactions generally have small neutron kerma factors and large photon production cross sections. Furthermore, in most cases these materials are of high atomic number, and they attenuate the photons effectively, resulting in a high ratio of gamma-ray to neutron heating. Therefore, in comparing the neutron kerma factors for various materials, it is not true in many cases that the material with the smallest k_n has the lowest nuclear heating; however, this is generally true for materials of the same (or nearly the same) atomic number.

In many cases, comparing the neutron kerma factors for several materials for the purpose of

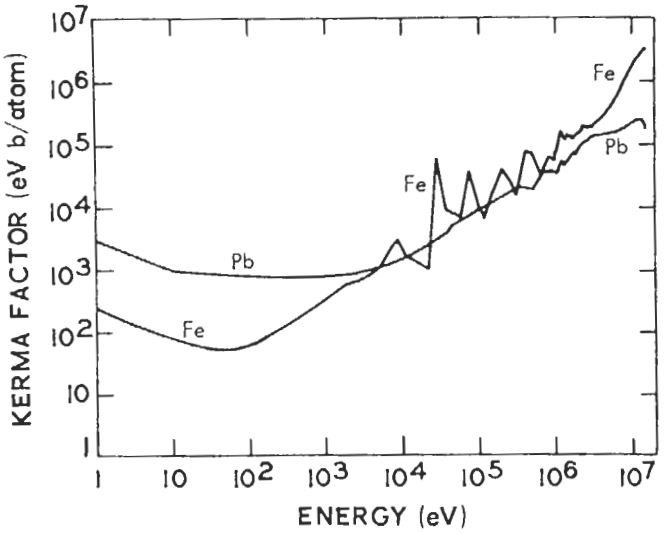

Fig. 8. Neutron kerma factor for iron and lead.

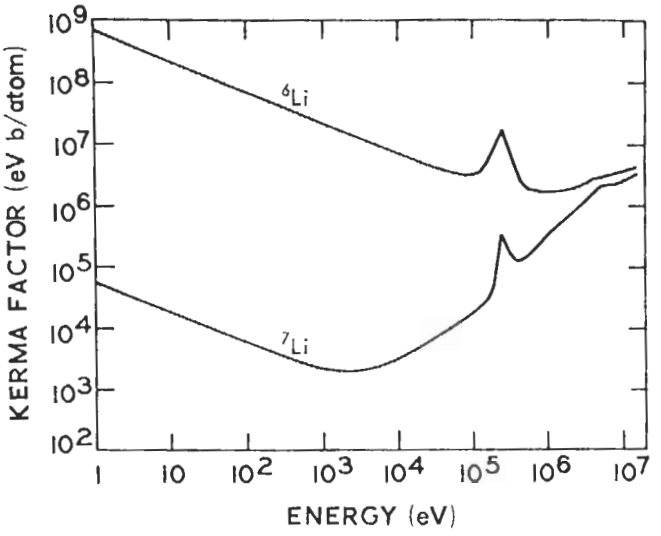

Fig. 10. Neutron kerma factor for ^{6}Li and ^{7}Li.

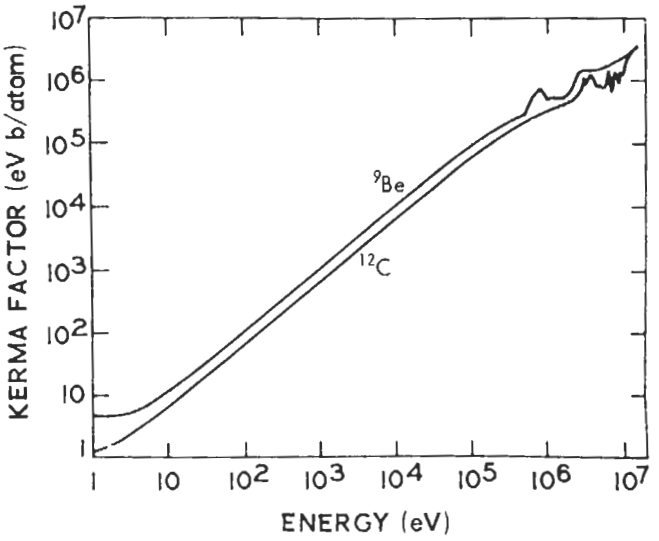

Fig. 9. Neutron kerma factor for ^{9}Be and ^{12}C.

comparing "energy multiplication" also does not yield useful results since the energies of the secondary neutrons and photons are not included in local energy deposition factors. Furthermore, k_n combines the energy release per reaction with the neutron reaction cross sections. Hence, a lower neutron kerma factor does not necessarily imply energy "gain" or "loss." For example, an endothermic (n, α) reaction usually yields a higher k_n than does the exothermic (n, γ) reaction.

A complete library of neutron kerma factors and reaction cross sections was generated for all materials for which nuclear data are available in ENDF/B-III. This library can be obtained from the Radiation Shielding Information Center at Oak Ridge National Laboratory.[21]

IV. VALIDITY OF NEUTRON KERMA-FACTOR RESULTS AND THE CONSISTENCY OF NUCLEAR DATA AND PROCESSING CODES

The models developed to calculate the kerma factors were used for generating data libraries, a sample of which has been presented. In the following, we address ourselves to the question of the validity of these results. The answer to this question can be divided into two parts. The first concerns the adequacy of the basic nuclear data from which neutron kerma factors were generated, and the second, the validity of the theoretical model and the correctness of the computations. The first part is difficult to answer, and a detailed investigation of the accuracy that can be assigned to presently available nuclear data is not discussed here. However, a sensitivity study of the neutron heating to basic nuclear data is carried out in another paper,[12] and the effect of the accuracy of particular types of data is determined. A general approach that provides an overall check on both the validity of the solutions of the kinematic equations and the correctness of the computations is developed next.

The main function of the kerma factors is in

[21] A complete library of pointwise and group kerma factors and reaction cross sections for 32 materials and isotopes generated with program MACK from ENDF/B data is available with documentation from the Radiation Shielding Information Center, Oak Ridge National Laboratory.

calculating the spatial distribution of nuclear heating in any system. The nuclear heating in a segment of the system is usually obtained by integrating the spatial distribution of the heating over the volume of the segment. However, the integral of the nuclear heating over a segment volume can be obtained, without using the kerma factors, from a direct energy balance for the segment (shown next).

Consider a segment of any nuclear system operating in a steady state. The net total neutron energy, L_{nE}, transported out of the segment can be written as

$$L_{nE}(\boldsymbol{r}_s) = \int_S \int_0^\infty E\, \boldsymbol{J}_n(\boldsymbol{r}_s, E) \cdot \boldsymbol{n}\, dE\, dS \quad , \quad (49)$$

and similarly for the gamma rays,

$$L_{\gamma E}(\boldsymbol{r}_s) = \int_S \int_0^\infty E\, \boldsymbol{J}_\gamma(\boldsymbol{r}_s, E) \cdot \boldsymbol{n}\, dE\, dS \quad , \quad (50)$$

where

S = surface of the segment

$\boldsymbol{n}$ = unit vector in the direction of the normal to that surface

$\boldsymbol{J}$ = net current.

Inside the segment, a gain or loss of kinetic energy occurs because of the exothermic and endothermic reactions in which conversion of kinetic energy into mass or vice versa takes place. External neutron and gamma-ray sources also might be present in the segment.

Let us define H_{nt} and $H_{\gamma t}$ as the total neutron and gamma-ray heating, respectively, in the segment, and $S_{E\gamma}$ as the total energy of the gamma rays produced in the segment from neutron-induced reactions. If we further define the parameter T_t as the sum of H_{nt} and $S_{E\gamma}$, then an energy balance for neutrons and photons yields

$$T_t = H_{nt} + S_{E\gamma} = - L_{nE} + \sum_j \sum_i R_{ij}\, Q_{ij} + \sum_j \sum_{i'} R_{i'j}\, E_{Di'j} + E_{sn} \quad (51)$$

$$H_{\gamma t} = - L_{\gamma E} + S_{E\gamma} + E_{s\gamma} \quad , \quad (52)$$

where

$$S_{E\gamma} = \sum_j \iiint N_j(\boldsymbol{r})\, \phi_n(\boldsymbol{r}, E_n) \times \sigma_p^j(E_n, E_\gamma) E_\gamma\, dE_n dE_\gamma\, d\boldsymbol{r} \quad , \quad (53)$$

and where

$N_j(\boldsymbol{r})$ = nuclide density of material j at $\boldsymbol{r}$

$\phi_n(\boldsymbol{r}, E_n)$ = neutron flux at neutron energy E_n and position $\boldsymbol{r}$

$\sigma_p^j(E_n, E_\gamma)$ = photon production cross section in element j for gamma rays of energy E_γ by neutrons of energy E_n

E_{sn} = total energy of the neutrons produced in the segment by external sources

$E_{s\gamma}$ = total energy of the gamma rays produced in the segment by external sources

R_{ij} = reaction rate (integrated over the segment volume) for reaction i in element j

Q_{ij} = Q value for reaction i in element j

$E_{Di'j}$ = decay energy per reaction i' in element j.

The subscript i is restricted to converting reactions in which the conversion of kinetic energy into mass or vice versa occurs.

Equations (51) and (52) provide a means of calculating the neutron and gamma-ray heating in a finite volume without using kerma factors. The sum of the neutron and gamma-ray heating can be obtained from Eqs. (51) and (52) once the results of the transport (hence, the subscript t in T_t and H_{nt}) calculations, namely reaction rates and surface currents, are known in addition to basic quantities such as the Q values. If the partition of the total heating to neutron and gamma-ray heating is desired, then $S_{E\gamma}$ must be known.

The method outlined above for calculating the heating integrated over a finite volume can now be used to check the results obtained with the kerma factors. Clearly, T_t in Eq. (51) must be equal to T_k:

$$T_t = T_k \quad , \quad (54)$$

where

$$T_k = H_{nk} + S_{E\gamma} \quad (55)$$

and

$$H_{nk} = \sum_j \iint N_j(\boldsymbol{r})\, \phi_n(\boldsymbol{r}, E_n)\, k_{nj}(E_n) dE_n\, d\boldsymbol{r} \quad ; \quad (56)$$

that is, T_k is the sum of the total neutron heating as calculated from the neutron kerma factors and $S_{E\gamma}$ as evaluated from Eq. (53). Assuming that the transport calculations are carried out correctly, Eq. (54) is a test of the consistency, using energy conservation as the criteria, of (a) the neutron interaction and transfer cross sections, (b) gamma-ray production cross sections, and (c) the neutron kerma factors. If this test is successfully satisfied, the validity of the neutron kerma factors in an integral sense is implicitly proven for the particular basic data set from which these parameters are derived.

For practical purposes, the multigroup energy representation is considered for carrying out the test of consistency in preserving the energy. This adds some uncertainty, since an effective neutron or gamma-ray energy must be known for each neutron and gamma-ray energy group. The effective energy for an energy group is a function of the energy limits of the group and the energy dependence of the flux within the group. In addition, an effective particle or photon energy for the group is implicitly assumed in generating multigroup cross sections and kerma factors through averaging over weighting spectra. Further discussion of this point is given in Ref. 22. A maximum deviation in calculating T_l and T_k with the data used in the following examples was estimated to be 3%.

To investigate the validity of the kerma-factor results obtained in this work, consider a fictitious system, *FS*, in slab geometry which consists of four spatial zones: (a) zone 1 is vacuum, (b) zone 2 is 5 cm thick, (c) zone 3 is 20 cm thick, and (d) zone 4 is 10 cm. We assume that one 14-MeV neutron is generated isotropically in the vacuum zone and that zones 2, 3, and 4 are filled with a material of nuclide density 0.05×10^{24} atom/cm^3. By using the ANISN code,[18] a 46-neutron-energy-group transport calculation was obtained for this system for several nuclides. The S_4 and P_1 approximations were used since the results of the energy balance check should be independent of the approximations utilized in generating the flux spectra. The multigroup cross sections were obtained from the DLC-2D library[23] which was generated from ENDF/B-III with the SUPERTOG code[24] using a $1/E$ weighting spectrum for the GAM-II 100-group structure. The DLC-2D data were properly collapsed into the 46-group form. The 46-group structure is the same as that of the GAM-II for the first 18 groups and has one broad group for each three groups of GAM-II at lower energies with the same thermal group. The gamma-ray production cross sections used in evaluating $S_{E\gamma}$ [see Eqs. (53) and (55)] came from ENDF/B-III for all materials except ^{6}Li and ^{7}Li which were taken from Ref. 7. Consistency in preserving the energy was investigated for several materials in zone 3 of the system described above. Tables IV and V show the results for ^{6}Li, ^{7}Li, ^{9}Be, and natural Fe. Table IV gives the Q values, decay energies per reaction, and reaction rates for all reactions in each material in zone 3 when zones 2, 3, and 4 are occupied with this material. Table V gives the individual terms of Eqs. (51) and (55) for each material. The neutron heating, H_{nk}, is calculated with neutron kerma factors obtained in the present work. All

[22]M. A. ABDOU, "Calculational Methods for Nuclear Heating and Neutronics and Photonics Design for CTR Blankets and Shields," PhD Thesis, University of Wisconsin, Nuclear Engineering Department, Madison, Wisconsin (1973); also, University Microfilms, Inc., No. 74-8981.

[23]R. Q. WRIGHT and R. W. ROUSSIN, "DLC-2/100 G Neutron Transport Cross Section Data Generated by SUPERTOG from ENDF/B3," RSIC data package DLC-2 (July 1973). This library can be obtained through the Radiation Shielding Information Center at Oak Ridge National Laboratory, Oak Ridge, Tennessee.

[24]R. Q. WRIGHT et al., "SUPERTOG: A Program to Generate Fine Group Constants and P_n Scattering Matrices from ENDF/B," ORNL-TM-2679, Oak Ridge National Laboratory (1969).

TABLE IV

Detailed Reaction Rates (in reactions per 14-MeV neutron) in Zone 3 of the Fictitious System (described in text) for ^{6}Li, ^{7}Li, ^{9}Be, and Fe

Reaction	Q Value (MeV)	E_D (MeV)	Reaction Rate, R	Reaction	Q Value (MeV)	E_D (MeV)	Reaction Rate, R
^{6}Li				^{7}Li			
$(n, 2n)$	-3.696	---	5.57361(-2)	$(n, 2n)$	-7.252	---	1.2373(-2)
$(n, n')d$	-1.471	---	6.8765(-1)	$(n, 2n)\alpha$	-8.723	---	1.6873(-2)
(n, γ)	+7.252	---	2.5290(-5)	$(n, n')t$	-2.466	---	4.8360(-1)
(n, p)	-2.733	1.560	1.5301(-2)	(n, γ)	+2.032	9.31	6.1471(-4)
$(n, \alpha)t$	+4.786	---	4.5550(-1)	(n, d)	-7.760	1.56	6.9051(-3)
^{9}Be				Fe (natural)			
$(n, 2n)$[a]	-1.660	0.095	8.6774(-1)	$(n, 2n)$	-11.204	---	1.3087(-1)
(n, γ)	+6.820	---	1.0267(-1)	(n, γ)	+7.803	---	1.7373(-1)
(n, p)	-12.830	6.24	4.4017(-5)	(n, p)	-2.7312	0.731	4.3209(-2)
(n, d)	-14.660	9.31	0.0	(n, α)	+0.3926	---	2.7646(-2)
(n, t)	-10.430	---	1.1990(-2)				
(n, α)	-0.600	1.56	8.0100(-2)				

[a]Combines all modes for which there are two neutrons and two alpha particles in the exit channel.

TABLE V

Individual Terms of Equations (51), (55), and (57) for ^{6}Li, ^{7}Li, ^{9}Be, and Fe in Zone 3 of the Fictitious System (described in the text)*

Material	Quantity							
	$-L_{nE}$	$\sum_i R_i Q_i$	$\sum_{i'} R_{i'} E_{Di'}$	T_t	$S_{E\gamma}$	H_{nk}[a]	T_k	$\%e = \frac{T_k - T_t}{T_t} \times 100$
^{6}Li	6.86649	+0.92084	0.02387	7.8112	0.12288	7.69049	7.8134	+0.023
^{7}Li	6.70721	-1.48181	0.01649	5.2407	0.62255	4.84930	5.4719	+4.41
^{9}Be	6.76980	-0.91391	0.20767	6.0636	0.51575	5.30736	5.8231	-3.97
Fe (natural)	6.06832	-0.21785	0.03159	5.8821	4.47670	1.37726	5.8540	-0.48

*All results normalized to one 14-MeV neutron in the source region, and all energies are in units of MeV.
[a]Neutron heating is derived with neutron kerma factors obtained in the present work.

results in Tables IV and V are normalized to one 14-MeV neutron in the vacuum zone, and all energies are in MeV. The quantities of interest given in Table V are T_t, T_k, and e. Definitions for T_t and T_k were given earlier; the parameter e is the error (or inconsistency in preserving the energy) and is defined as

$$e = \frac{T_k - T_t}{T_t} \quad . \tag{57}$$

Table V shows that e is about 0.02, 4.4, -4.0, and -0.5% for ^{6}Li, ^{7}Li, ^{9}Be, and natural Fe, respectively. The error in ^{6}Li and natural Fe is very small and is mainly due to approximating the effective energy per group. While 2 to 3% of the error in ^{7}Li and ^{9}Be can be associated with the use of the midpoint energy of a group as its effective energy, 1 to 2% is an actual inconsistency in preserving the energy between (a) neutron multigroup cross sections, (b) neutron kerma factors, and (c) gamma-ray production cross sections. Although such an error is small, it was further investigated,[22] and it was concluded that it occurs because of inconsistencies in basic neutron interaction and gamma-ray production data rather than in the calculational algorithms for neutron kerma factors and gamma-ray production cross sections. Because nuclear data are not very well known at present, neutron interaction data may be available for some reactions for which gamma-ray production information is not known, or vice versa. In addition, the gamma-ray production information inevitably relies heavily on references and measurements different from those used for the neutron interaction data, and such discrepancies in preserving the energy can be expected.

In calculating nuclear heating, the total heating is usually of greatest concern rather than the exact partitioning into neutron and gamma-ray heating. A slight increase or decrease in the neutron heating, with a corresponding adjustment in the gamma-ray production data to preserve the energy, results in a slight change in only the spatial dependence of nuclear heating, but the integral over a finite volume will be much more accurate. The perfection of both neutron interaction and secondary gamma-ray production data cannot be achieved today and is not likely to be possible in the near future. Therefore, a compromise solution can be sought in light of the above discussion by processing the photon production matrix simultaneously with the neutron kerma factors. This allows the development of a scheme to preserve the energy and provide more consistent nuclear parameters.

From the results of this section and several similar studies for other materials, the validity of the neutron kerma factors calculated in this work is verified in an integral sense. This verification is only for the overall correctness of the theoretical model and the computations of the kerma factors for a given set of nuclear data. This method of verification, however, does not guarantee the absence of compensation for error in the various energy ranges and does not answer the question of the adequacy of the basic nuclear data from which the kerma factors were calculated. The question of the basic nuclear data is discussed in the sensitivity study given in another paper.[12] Pointwise verification of the results was carried out for several cases by a direct calculational check.

V. COMPARISON WITH PREVIOUS WORK

As mentioned earlier, several efforts have previously been made to calculate neutron kerma factors.[2-7] A comparison of the neutron kerma factors calculated here with previous work is appropriate.

Most of the previous work was directed toward elements that are major constituents in the human body. Several simplifying assumptions were usually employed in some of this earlier work, the most notable of these being the following:

1. neglecting the total contribution of some important reactions
2. ignoring the anisotropy of elastic scattering
3. failing to include the resonance contribution of appropriate reaction cross sections in several cases
4. inadequately treating the partitioning of the energy deposition and secondary neutron and photon emission.

In addition, none of the previous works had a general format or computational algorithm for calculating neutron fluence-to-kerma factors; the same effort had to be duplicated for each material or for a new revision of the basic nuclear data for the same material.

The most recent ENDF/B data[10,11] and in some cases the United Kingdom data[13] were used for calculating the neutron kerma factors presented here. The evaluations of these libraries are far from perfect, as will be noted in another paper[12]; however, due to the extensive efforts expended in preparing and revising these evaluations and due to their wide usage,[25] they represent the most and presumably best data available. Thus, it is fair to say that the neutron kerma factors presented are calculated to the best of our present knowledge of nuclear data.

The most recent and extensive among the previous works is that of Ritts et al.,[6,7] who made a real attempt to include a large number of significant reactions for several materials. However, their work had several drawbacks which greatly affected the accuracy of their kerma-factor results:

1. They assumed[6,7] the evaporation model to be valid in all cases for describing the secondary neutron energy distribution from inelastic scattering to continuum and $(n,2n)$ reactions. This assumption is known to be invalid in several cases, e.g., in the ^{9}Be $(n,2n)$ reactions. (The present work allows for a general format for describing the secondary neutron energy spectra.)

2. They assumed[6] that the nuclear temperature for this evaporation model can be calculated from the Fermi gas model which predicts the nuclear temperature, θ, as $\theta(E) = (10E/A)^{1/2}$, where E and θ are in MeV. This relation is very approximate, particularly for magic or near magic and light nuclei.

3. The Ritts et al. treatment of the inelastic scattering to the continuum yields particularly poor results for the following reasons: They always incorporated the evaporation model for representing the secondary neutron energy spectra which, if adequate, is valid only for *true* inelastic scattering to continuum, i.e., when the residual nucleus is left in the continuum energy range. However, the nuclear data they used combine all modes of inelastic scattering (level and continuum) for incident energies above a certain energy (in rather arbitrary fashion in most cases), and the combined cross sections are identified as the cross sections for inelastic scattering to the continuum, regardless of the state of the residual nucleus. Consequently, the secondary energy distribution in such cases includes the discrete spectrum from level scattering, and the use of an evaporation model for this secondary neutron spectrum yields poor results for the average energy of the secondary neutron. Furthermore, the solution of Ritts et al.[6,7] of the kinematics equations for inelastic scattering to the continuum relies on using the quantity Q_{min}, which is the Q value for the minimum excitation energy for the continuum range in the residual nucleus. Since the data they used had a different definition of inelastic scattering to the continuum, Q_{min} was given as zero in most of their nuclear data. Given the fact that Q_{min} is typically a few MeV, it is clear that the neutron kerma factors they calculated were not correct in such cases. (For this reason, the present work has intentionally avoided incorporating any Q value into the calculations for inelastic scattering to the continuum. Rather, an accurate calculation of the known secondary neutron energy spectra was employed.)

4. In several cases, the anisotropy of elastic scattering was entirely ignored in the work of Ritts et al.[6,7] This resulted in very poor kerma factors, particularly in the high-energy range, as will be shown shortly. (Here, the anisotropy of both elastic and inelastic scattering is treated as accurately as the data permit.)

5. Some evaluations of nuclear data used by Ritts et al. (05R and ENDF/B-I and -II) provided the resonance parameters for the resonance region, and the smooth cross sections given in this

[25] R. Q. WRIGHT, S. N. CRAMER, and D. C. IRVING, "UKE-III: A Computer Program for Translating Neutron Cross Section Data from the UKAEA Nuclear Data Library to the Evaluated Nuclear Data File Format," ORNL-TM-2880 (rev.), Oak Ridge National Laboratory (1973); also see ENDF-134 R.

range were the background cross sections only. Due to the lack of a resonance treatment in the Ritts technique, the contribution of the resonance cross sections was ignored in such cases. This affected their kerma factor results for elastic scattering and radiative capture in the resonance region. (The MACK program developed in the present work has a built-in capability for calculating the contribution from both the resolved and unresolved regions, including the effect of Doppler broadening.)

6. Ritts et al. made no attempt to calculate the excitation energy of the residual nucleus from the $(n,2n)$ reaction, and the gamma-ray energy emission from this reaction was ignored; that is, the emission was implicitly assumed to be deposited locally. This can be clearly seen from Eq. (17) in Ref. 6 and Eq. (12) in Ref. 7. [In the present work the excitation energy of the residual nucleus is calculated from Eq. (33)].

The above discussion clearly indicates that because of the assumptions in the calculational and processing models, large differences between the neutron kerma-factor results obtained here and those calculated by Ritts et al.[6,7] can be expected even if the nuclear data used in both works are the same. In addition, due to frequent changes in basic nuclear data from one evaluation to another, the nuclear data used by Ritts et al. (05R and ENDF/B-I and -II libraries) several years ago are different in many instances from the nuclear data used in the present work (ENDF/B-III).

Tables VI, VII, and VIII compare the neutron kerma factors obtained in the present work with those of Ritts et al.[6,7] for ^{7}Li, Be, and ^{23}Na. These tables show that the difference between the results is large, particularly in the 5- to 15-MeV range where the difference is more than 50%.

In calculating the sodium kerma factors, Ritts et al.[6,7] included only elastic and inelastic scattering and radiative capture. The present work included, in addition to these reactions, the (n,p), (n,α), and $(n,2n)$ reactions. The contribution of these latter reactions to the ^{23}Na kerma factor is

TABLE VI

Comparison of Neutron Kerma Factors Obtained from the Present Work and from the Data of Ritts et al. (Refs. 6 and 7) for Lithium-7

Energy (eV)	Mack (A) (erg b/ atom)	Ritts et al. (B) (erg b/atom)	Percentage Difference $\frac{B-A}{A}\times 100$
15.00 (+6)[a]	5.5610 (-6)	8.4077 (-6)	+51.19
13.74 (+6)	5.2127 (-6)	8.1303 (-6)	+55.97
12.58 (+6)	4.9426 (-6)	7.7682 (-6)	+57.17
11.52 (+6)	4.7118 (-6)	7.4047 (-6)	+57.15
10.06 (+6)	4.3100 (-6)	6.6240 (-6)	+53.69
9.08 (+6)	3.9599 (-6)	5.9849 (-6)	+51.14
8.10 (+6)	3.6304 (-6)	5.3451 (-6)	+47.23
7.19 (+6)	3.4451 (-6)	4.7421 (-6)	+37.64
6.05 (+6)	3.5092 (-6)	4.0888 (-6)	+16.51
5.16 (+6)	3.2791 (-6)	3.6657 (-6)	+11.79
4.08 (+6)	2.8070 (-6)	2.8084 (-6)	+0.05
3.18 (+6)	1.9212 (-6)	1.9025 (-6)	-0.97
2.01 (+6)	1.1483 (-6)	1.1252 (-6)	-2.01
1.55 (+6)	8.7685 (-7)	8.6984 (-7)	-0.79
1.07 (+6)	6.0570 (-7)	5.9150 (-7)	-2.34
7.88 (+5)	4.1466 (-7)	4.0516 (-7)	-2.29
2.57 (+5)	9.2739 (-7)	9.3050 (-7)	+0.33
1.17 (+5)	3.1988 (-8)	2.7903 (-8)	-12.77
5.73 (+4)	1.8157 (-8)	1.5379 (-8)	-15.29
1.37 (+4)	6.1561 (-9)	4.7871 (-9)	-22.24
1.02 (+3)	3.3403 (-9)	3.7655 (-10)	-88.72
5.46 (+1)	1.1955 (-8)	1.9531 (-8)	+63.37
9.16 (+0)	2.8068 (-8)	4.5971 (-8)	+63.78
1.00 (+0)	8.6508 (-8)	1.4156 (-7)	+63.63

[a]Read as 15.00×10^{6}.

TABLE VII

Comparison of Neutron Kerma Factors Obtained from the Present Work and from the Data of Ritts et al. (Refs. 6 and 7) for Beryllium

Energy (eV)	Mack (A) (erg b/atom)	Ritts et al. (B) (erg b/atom)	Percentage Difference $\frac{B-A}{A}\times 100$
15.00 (+6)[a]	6.2053 (-6)	1.1918 (-5)	+92.06
13.74 (+6)	0.54154 (-5)	1.1609 (-5)	+114.30
12.58 (+6)	0.48806 (-5)	1.0955 (-5)	+124.40
11.52 (+6)	0.4334 (-5)	1.0369 (-5)	+139.30
10.06 (+6)	3.8381 (-6)	9.2613 (-6)	+141.30
9.08 (+6)	3.5878 (-6)	8.5437 (-6)	+138.10
8.10 (+6)	3.3678 (-6)	7.8777 (-6)	+133.90
7.19 (+6)	3.1346 (-6)	6.9825 (-6)	+122.70
6.05 (+6)	2.9031 (-6)	5.9107 (-6)	+103.50
5.16 (+6)	2.6148 (-6)	5.0177 (-6)	+91.89
4.08 (+6)	2.3722 (-6)	3.8639 (-6)	+62.88
3.18 (+6)	2.3402 (-6)	3.2239 (-6)	+37.76
2.01 (+6)	1.1102 (-6)	1.0273 (-6)	-7.46
1.55 (+6)	8.1354 (-7)	7.6024 (-7)	-6.55
1.07 (+6)	8.2838 (-7)	8.6286 (-7)	+4.16
7.88 (+5)	7.4371 (-7)	7.5710 (-7)	+1.80
2.57 (+5)	3.1838 (-7)	3.2117 (-7)	+0.87
1.17 (+5)	1.7944 (-7)	1.7622 (-7)	-1.79
5.73 (+4)	9.5500 (-8)	9.2990 (-8)	-2.62
1.37 (+4)	2.3833 (-8)	2.3022 (-8)	-3.40
1.02 (+3)	1.7825 (-9)	1.7159 (-9)	-3.73
5.46 (+1)	9.6003 (-11)	9.2855 (-11)	-3.27
9.16 (+0)	1.7957 (-11)	1.7778 (-11)	-0.99
1.00 (+0)	7.8243 (-12)	9.0808 (-12)	+16.05

[a]Read as 15.00×10^{6}.

roughly 75% in the high-energy range. This accounts for most of the difference between their work and ours.

For the cases of ^{7}Li and Be, the reactions included in both works are the same, and investigation of the adequacy of the two works is appropriate. In the last section a method was developed for investigating the consistency of the neutron kerma-factor results in preserving the energy by comparing the neutron heating rate obtained from these kerma factors with that obtained from an energy balance over a finite volume of space for which the neutron flux and surface current are known. The method was then used to verify the results of the present work for several materials, including ^{7}Li and Be, as shown in Tables IV and V. Similar calculations were further carried out with the neutron kerma factors obtained by Ritts et al.,[7] and the results are shown in Table IX. These results indicate that using the Ritts et al. kerma factors destroys the energy balance, with an error of roughly 40% for ^{7}Li and 70% in the case of Be.

TABLE VIII

Comparison of Neutron Kerma Factors Obtained from Present Work and from Ritts et al. Data for Sodium

Energy (eV)	Mack (A) (erg b/atom)	Ritts et al. (B) (erg b/atom)	Percentage Difference $\frac{B-A}{A}\times 100$
15.00 (+6)[a]	4.8781 (-6)	1.3787 (-6)	-72.00
13.74 (+6)	4.9535 (-6)	1.3001 (-6)	-74.00
12.58 (+6)	4.9771 (-6)	1.1905 (-6)	-76.00
11.52 (+6)	4.5227 (-6)	1.1133 (-6)	-75.00
10.06 (+6)	3.8837 (-6)	9.9110 (-7)	-74.00
9.08 (+6)	2.4656 (-6)	8.6723 (-7)	-65.00
8.10 (+6)	2.0279 (-6)	8.2005 (-7)	-59.00
7.19 (+6)	1.3328 (-6)	7.6774 (-7)	-42.00
6.05 (+6)	1.0607 (-6)	7.7151 (-7)	-27.00
5.16 (+6)	8.3001 (-7)	7.7395 (-7)	-6.75
4.08 (+6)	7.2651 (-7)	6.6941 (-7)	-7.86
3.18 (+6)	6.1180 (-7)	5.6253 (-7)	-8.05
2.01 (+6)	4.7496 (-7)	5.4073 (-7)	+13.84
1.55 (+6)	3.1112 (-7)	3.7786 (-7)	+21.45
1.07 (+6)	4.529 (-7)	4.9608 (-7)	+9.53
7.88 (+5)	4.3213 (-7)	5.0191 (-7)	+16.15
2.57 (+5)	1.1632 (-7)	1.0345 (-7)	-11.06
1.17 (+5)	5.3342 (-8)	4.9424 (-8)	-7.34
5.73 (+4)	3.3171 (-8)	4.4720 (-8)	+34.81
1.37 (+4)	8.1779 (-9)	9.2012 (-9)	+12.50
1.02 (+3)	8.5143 (-9)	4.2942 (-9)	-49.56
5.46 (+1)	10.5491 (-9)	7.5355 (-9)	-28.56
9.16 (+0)	2.5090 (-8)	1.8581 (-8)	-25.90
1.00 (+0)	7.5943 (-8)	5.6718 (-8)	-25.31

[a]Read as 15.00×10^{6}.

VI. CONCLUSIONS

A theoretical model was developed for calculating fluence-to-kerma factors from basic nuclear data. No major simplifying assumptions were introduced, and the accuracy of the calculated kerma factors depends only on the availability and accuracy of the basic nuclear data. A computer program called MACK was written to calculate kerma factors from nuclear data in ENDF format. A library of kerma factors and partial group cross sections was generated with MACK for all materials of interest in nuclear applications. The program and libraries are available from the Radiation Shielding Information Center at Oak Ridge National Laboratory.

An algorithm was also developed for investigating the validity of the kerma factors by using an integral energy balance. The validity of the

TABLE IX

Comparison of the Consistency in Preserving the Energy Using Neutron Kerma Factors Obtained in the Present Work and Those Obtained by Ritts et al. (Ref. 7) for Several Materials in Zone 3 of the Fictious System *

Material	$S_{E\gamma}$ (Total Gamma-Ray Energy Produced)	$T_t = H_{nt} + S_{E\gamma}$ (Predicted from Transport Calculations)	Neutron Heating (H_{nk}) Using Kerma Factor from		$T_k = H_{nk} + S_{E\gamma}$		$e = \frac{T_k - T_t}{T_t}\times 100$	
			Present Work	Ritts et al. (Ref. 7)	Present Work	Ritts et al. (Ref. 7)	Present Work	Ritts et al. (Ref. 7)
^{6}Li	0.12288	7.8112	7.69049	8.37586	7.8134	8.4987	+0.023	+8.80
^{7}Li	0.62255	5.2407	4.84930	6.72248	5.4719	7.3450	+4.41	+40.15
^{9}Be	0.51575	6.0636	5.30736	9.92152	5.8231	10.4373	-3.97	+72.13
Fe	4.47670	5.8821	1.37726	1.11208	5.8540	5.58878	-0.48	-4.99

*Results are normalized to one 14-MeV neutron in the source region. All energies are in MeV.

theoretical model and the correctness of the computation of the kerma factors obtained in the present work were verified using this algorithm. Comparison of these kerma-factor results with previous work showed that they provide a considerable improvement in kerma-factor and nuclear-heating calculations.

It was also shown that there is some inconsistency in preserving the energy between the basic neutron interaction and gamma-ray production data. Since the perfection of both neutron interaction and secondary gamma-ray production data is very difficult at present, it is suggested that to ensure consistency, the photon-production cross-section matrix be processed simultaneously with neutron kerma factors.